Eur. Phys. J. C 56, 33–38 (2008)
DOI 10.1140/epjc/s10052-008-0633-3

THE EUROPEAN PHYSICAL JOURNAL C

Regular Article – Theoretical Physics

Diffractive photoproduction of Z^0 bosons in coherent interactions at CERN-LHC

V.P. Gonçalves[1], M.V.T. Machado[2,a]

[1] Instituto de Física e Matemática, Universidade Federal de Pelotas, Caixa Postal 354, CEP 96010-090, Pelotas, RS, Brazil
[2] Centro de Ciências Exatas e Tecnológicas, Universidade Federal do Pampa, Campus de Bagé, Rua Carlos Barbosa, CEP 96400-970, Bagé, RS, Brazil

Received: 17 January 2008 / Revised version: 27 April 2008 /
Published online: 5 June 2008 –

Abstract. Exclusive Z^0 photoproduction at high energies in $\gamma p(A)$, pp and AA collisions is investigated within the color dipole formalism. We generalize the description of the deeply virtual Compton scattering (DVCS) process, which describes the HERA data quite well, for the production of Z^0 bosons and estimate the total cross section for the exclusive process $\gamma^* h \to Z^0 h$ ($h = p, A$) for different energies, photon virtualities and atomic numbers. As hadrons at collider energies are a source of Weizsäcker–Williams photons, we consider electromagnetic interactions in hadron–hadron collisions at Tevatron and LHC energies and estimate the rapidity distribution and the total cross section for Z^0 production in the $hh \to hZ^0h$ process. This may allow us to study, for instance, the physics of hadronic Z^0 decays in a clean environment characterized by two rapidity gaps. Our results indicate that the experimental analyses of this process could be feasible in pp, but the physics scenario for AA collisions is not promising.

PACS. 12.38.-t; 12.38.Bx; 14.70.Hp

1 Introduction

The Large Hadron Collider (LHC) at CERN will explore physics at TeV scale, opening a new territory, where ground breaking discoveries are expected [1, 2]. One primary goal of the LHC is the search and study of the properties of the Higgs boson, which is motivated by the determination of the electroweak symmetry breaking mechanism and discrimination among the physics models beyond the standard model (SM). Recently, there has been a great deal of attention devoted to study of the central exclusive diffractive (CED) Higgs boson production, $h_1h_2 \to h_1 \otimes H \otimes h_2$, where $\otimes$ is a rapidity gap in the final state, characterized by no activity between the outgoing hadrons and the decay products of the Higgs boson, i.e. by a clean experimental signature (for a recent review see, e.g., [3]).

Another interesting physics signal as well as an important background to a number of processes indicating the presence of new physics is the production of the Z^0 boson [4]. It should be produced copiously in pp and AA collisions at LHC, decaying afterwards into lepton pairs or hadrons (see, e.g., [5]). However, the hadronic Z^0 decays are expected to be difficult to identify, due to the overwhelming background of QCD multi-jet production, owing to the hadronic event environment. It implies that in pp collisions it is almost impossible to study the physics of hadronic Z^0 decays. Consequently, although the LHC can be considered a Z^0 factory, it only allows for high-statistics measurement in final states with leptons. In this letter we propose an alternative to produce Z^0 bosons and study the related physics from hadronic Z^0 decays in a clean environment characterized by two rapidity gaps between the Z^0 and the outgoing hadrons, which can be detected in the forward proton detectors proposed in the CMS and ATLAS experiments at LHC. Basically, we propose to study the diffractive Z^0 photoproduction in coherent hadron–hadron interactions. This process is characterized by the photon–hadron interaction, with the photon stemming from the electromagnetic field of one of the two colliding hadrons (for recent reviews see [6, 7]). The Z^0 is produced when the photon fluctuates into a quark–antiquark ($q\bar{q}$) pair, scatters diffractively on the target hadron through gluon exchanges, and emerges as a Z^0. The Z^0 mass provides the hard scale that justifies a perturbative calculation. The total cross section for the $hh \to h \otimes Z^0 \otimes h$ process is given by

$$\sigma\left(h_1h_2 \to h_1Z^0h_2\right) = \int_{\omega_{\rm min}}^{\infty} {\rm d}\omega \frac{{\rm d}N_\gamma(\omega)}{{\rm d}\omega} \sigma_{\gamma h \to Z^0 h}\left(W^2_{\gamma h}\right), \tag{1}$$

where ω is the photon energy and $\frac{{\rm d}N_\gamma(\omega)}{{\rm d}\omega}$ is the equivalent flux of photons from a charged hadron. Moreover,

[a] e-mail: magnus@if.ufrgs.br

$\omega_{\rm min} = M_{Z^0}^2/4\gamma_{\rm L} m_p$, $\gamma_{\rm L}$ is the Lorentz boost of a single beam, $W_{\gamma h}^2 = 2\omega\sqrt{S_{NN}}$ and $\sqrt{S_{NN}}$ is the c.m.s. energy of the hadron–hadron system [6, 7]. This process is characterized by small momentum transfer and energy loss, which implies that the outgoing hadrons should be detected in the forward regions of the main LHC detectors. The study of this process is feasible considering the proton tagging detectors (Roman pots) already planned for the initial start-up of the LHC in the 220–240 m region by CMS/TOTEM and ATLAS. Moreover, the situation can still be improved in the future if the Roman pots at 420 m from the interaction points of ATLAS and/or CMS were installed (for details see, e.g., [8–10]).

One has that the cross section for Z^0 production, (1), is directly dependent of the magnitude and energy dependence of the $\gamma h \to Z^0 h$ cross section, which is currently unknown. Here, we estimate this cross section considering a generalization of the dipole picture approach [11–13] currently used for the description of deep virtual Compton scattering (DVCS) in ep collisions at HERA [14–20]. Specifically, in this approach the exclusive process $\gamma p \to Ep$ is described by the interaction of $q\bar{q}$ pairs (color dipoles), that the virtual boson fluctuate into, with the nucleon. The scattering amplitude is given by the convolution of the dipole–nucleon cross section with the overlap of the virtual incoming boson and outgoing exclusive (E) final state wave functions. This approach provides a very good description of the data on γp inclusive production, $\gamma\gamma$ processes, diffractive deep inelastic and vector meson production (see, e.g., [17]). As the wave functions and dipole–target cross section are reasonably well known, one sees that our calculation of the diffractive Z^0 photoproduction introduces no new parameters. Therefore, the Z^0 production in γh interactions can be considered as an important test of the dipole approach formalism as well as a search of information about the dipole–target cross section and, consequently, of the QCD dynamics at high energies.

2 Diffractive production of Z^0 at high energies

Let us introduce the main formulas concerning the color dipole picture applied to the exclusive processes in deep inelastic scattering (DIS). In the dipole model [11–13], DIS is viewed as the interaction of a color dipole, i.e., mostly a quark–antiquark pair, with the target. The transverse size of the pair is denoted by $\mathbf{r}$ and a quark carries a fraction z of the photon's light-cone momentum. In the target rest frame, the dipole lifetime is much longer than the lifetime of its interaction with the target. Therefore, elastic $\gamma^* h$ scattering is assumed to proceed in three stages: first the incoming virtual photon fluctuates into a quark–antiquark pair, then the $q\bar{q}$ pair scatters elastically on the target, and finally the $q\bar{q}$ pair recombines to form the exclusive final state (real photons, vector mesons, flavor mesons, etc.). The amplitude for the elastic process $\gamma^* h \to \gamma^* h$, $\mathcal{A}^{\gamma^* h}(x, Q, \Delta)$, is simply the product of the amplitudes of these three subprocesses integrated over the dipole variables $\mathbf{r}$ and z:

$$\mathcal{A}^{\gamma^* h}(x, Q, \Delta) = \sum_f \sum_{n,\bar{n}} \int {\rm d}^2\mathbf{r} \int_0^1 {\rm d}z \Psi^*_{n\bar{n}}(r, z, Q) \times \mathcal{A}_{q\bar{q}}(x, r, \Delta) \Psi_{n\bar{n}}(r, z, Q)\,, \qquad (2)$$

where $\Psi_{n\bar{n}}(r, z, Q)$ denotes the amplitude for the incoming virtual photon to fluctuate into a quark–antiquark dipole with helicities n and $\bar{n}$ and flavor f. The quantity $\mathcal{A}_{q\bar{q}}(x, r, \Delta)$ is the elementary amplitude for the scattering of a dipole of size $\mathbf{r}$ on the proton, Δ denotes the transverse momentum lost by the outgoing proton (with $t = -\Delta^2$), x is the Bjorken variable, and Q^2 is the photon virtuality. Equation (2) has been extensively used to compute the $\gamma^* p$ cross section and the proton structure functions as well (see, e.g., [17, 21]). On the other hand, the amplitude for production of an exclusive final state, E, is given by [21]

$$\mathcal{A}^{\gamma^* h \to Eh}(x, Q, \Delta) = \int {\rm d}^2\mathbf{r} \int_0^1 {\rm d}z (\Psi^*_E \Psi_{\gamma^*}) \mathcal{A}_{q\bar{q}}(x, r, \Delta)\,, \qquad (3)$$

where $(\Psi^*_E \Psi_{\gamma^*})$ denotes the overlap of the virtual incoming photon and outgoing exclusive final state E wave functions (non-forward wave functions will be used [22]). Consequently, the elastic diffractive cross section is given by

$$\frac{{\rm d}\sigma^{\gamma^* h \to Eh}}{{\rm d}t} = \frac{1}{16\pi} |\mathcal{A}^{\gamma^* h \to Eh}(x, Q, \Delta)|^2\,. \qquad (4)$$

For the elementary dipole–proton amplitude, $\mathcal{A}_{q\bar{q}}(x, r, \Delta)$, we will consider the saturation model proposed in [20], which describes quite well the current HERA data for exclusive processes. It is based on saturation physics, which predicts the limitation on the maximum phase-space parton density that can be reached in the hadron wave function (parton saturation) and the transition between the linear and nonlinear regimes of the QCD dynamics at high energies. This transition is specified by a typical scale, which is energy dependent and is called the saturation scale $Q_{\rm sat}$ (for a review see [23–25]). In the model considered the elementary dipole–proton amplitude is given by [20]

$$\mathcal{A}_{q\bar{q}}(x, r, \Delta) = 2\pi R_p^2 F(\Delta) N(r Q_{{\rm sat},p}(x, |t|), x)\,, \qquad (5)$$

which is an extension of the forward model [26] including the QCD predictions for non-zero momentum transfer, which reproduces the initial model for $|t| = 0$ and ensures that the saturation scale has the correct asymptotic behaviors. The dipole–nucleon scattering amplitude at $t = 0$ is given by

$$N(x, r) = \begin{cases} \mathcal{N}_0 \left(\frac{rQ_{\rm sat}}{2}\right)^{2\left(\gamma_s + \frac{1}{\kappa\lambda Y} \ln \frac{2}{rQ_{\rm sat}}\right)}\,, & rQ_{\rm sat} \le 2\,, \\ 1 - {\rm e}^{-A \ln^2(BrQ_{\rm sat})}\,, & rQ_{\rm sat} > 2\,, \end{cases} \qquad (6)$$

where $Y = \ln(1/x)$, and the parameters are $\mathcal{N}_0 = 0.7$, $\kappa = 9.9$ and $\gamma_s = 0.63$. The constants A and B are obtained from the continuity conditions at $rQ_{\rm sat} = 2$. The

t dependence of the saturation scale is parameterized as $Q^2_{\rm sat,}{}_p(x,|t|) = Q_0^2(1+c|t|)x^{-\lambda}$, in order to interpolate smoothly between the small and intermediate transfer regions. The form factor $F(\Delta) = \exp(-B|t|)$ catches the transfer dependence of the proton vertex, which is factorized from the projectile vertices and does not spoil the geometric scaling properties. Finally, the scaling function N is obtained from the forward saturation model [26]. The remaining parameters are $Q_0 = 0.206\,\text{GeV}$, $\lambda = 0.253$, $c = 3.776\,\text{GeV}^{-2}$ and $B = 3.74\,\text{GeV}^{-2}$.

In the case investigated here, we have exclusive production of Z at the final state, $E = Z^0$. Therefore, the non-forward scattering amplitude will be given by (3), with the overlap of the incoming virtual photon and outgoing Z^0 final state wave functions, $(\Psi^*_{Z^0}\Psi_{\gamma^*})$. Regarding the wave functions, the Z^0 bosons behave in the same way as the photon, which implies that we can use the result from [22], and only the magnitude of the coupling to the quarks depends on the nature of the boson [27]. The scale in the Z^0 wave function is given by its mass for on-shell production. Explicit expressions for the boson wave functions can be found e.g. in [28, 29]. Namely, the light-cone wave functions for a virtual Z boson can be obtained from the photon wave function by the replacement $e_Q\gamma_\mu \to (g_W/2\cos\theta_{\rm W})\gamma_\mu(c_V - c_A\gamma_5)$.

Some comments are in order at this point. Firstly, it is important to emphasize that due to the large mass of the Z^0, the $q\bar{q}$ dipole is spatially compact, which implies that the cross section is dominated by small pair separations, i.e. by the linear regime of the QCD dynamics. That is, the mean color dipole radius is of order $r \propto 1/m_Z \ll 1/Q_{\rm sat}$. Concerning the saturation effects, its contribution is more sizeable at large dipole configurations, meaning that for Z^0 production we should expect that the associated modifications will be small. This is corroborated by the numerical calculations presented in what follows, where the effective energy power law for Z production is of order $\lambda_{\rm eff} \simeq 0.5$. Such an effective power is clearly consistent with BFKL-like QCD dynamics for the process, and gluon resummation effects are not very important. Our calculation is consistent with BFKL dynamics as the employed saturation model of [26] reproduces the BFKL QCD regime for small color dipoles. Since such an approach provides a very good description of the diffractive and inclusive HERA data, including the DVCS experimental data, and the description does not include any new parameter, one is led to believe that our predictions are reasonable for LHC energy.

Secondly, it is timely to discuss related approaches for the present scattering process and to discuss to what extent they could differ from the current calculation. We quote the pioneering work of [30] (denoted BL hereafter), where an analysis using non-forward QCD planar ladder diagrams has been considered to compute the diffractive Z^0 production in an ep collider. The computation allows for QCD evolution in the low-x region; however, a direct comparison to ours results is a hard task. As an estimation, a cross section $\sigma \approx 10^{-37}\,\text{cm}^2$ is found after including the branching ratio for the μ-decay [30]. This means a cross section $\sigma_{\rm BL}(ep \to Z^0 ep) \approx 3\,\text{pb}$, which leads to $\sigma_{\rm BL}(\gamma p \to Z^0 p)$ being about 0.01 pb at $\sqrt{s} = 300\,\text{GeV}$, consistent with the present work. In [31], the two-gluon exchange model of the pomeron is used to compute the Z^0 photoproduction, where reggeization of the gluons and interactions between them (ladder diagrams) are ignored. The main uncertainties in that calculation are the parameterization for the gluon–proton amplitude and the finite gluon mass included in the propagators to suppress long distance contributions. The integrated cross section (energy independent) is $\sigma_{2g}(\gamma p \to Z^0 p) \simeq 0.025\,\text{pb}$, with an uncertainty factor of 2 [31]. This value is consistent with our calculations for $\sqrt{s} \gg m_Z$. Finally, it would be interesting to compare this work with a conventional partonic description of timelike Compton scattering. Presently, the photoproduction of a heavy timelike photon that decays into a lepton pair, $\gamma p \to l^+ l^- p$, is computed to leading twist and at Born level [32]. In our case, the virtual photon in the final state is replaced by the weak neutral boson. The amplitude is given by the convolution of hard scattering coefficients, calculable in perturbation theory, and generalized parton distributions (GPDs), which describe the nonperturbative physics of the process. For instance, in [32], the quark handbag diagrams (leading order in $\alpha_{\rm s}$) and simple models of the relevant GPDs are used to estimate the cross section and the angular asymmetries for lepton pair production. In the coherent case (real photons from proton or nuclei) studied here, the background from a Bethe–Heitler process can be completely disregarded. We remark that such a calculation cannot be compared with ours, since an explicit analysis using $\mathcal{O}(\alpha_{\rm s})$ accuracy, one-loop corrections to the quark handbag diagrams and other diagrams involving gluon distributions is currently unknown.

We are now ready to compute the total cross section. In Fig. 1 we present the calculation for the total cross section (integrated over $|t| \leq 1$) as a function of energy for distinct photon virtualities. The range of energy is extrapolated up to $W_{\gamma p} = 1\,\text{TeV}$. It is verified that the cross section is weakly dependent on the virtuality, due to the

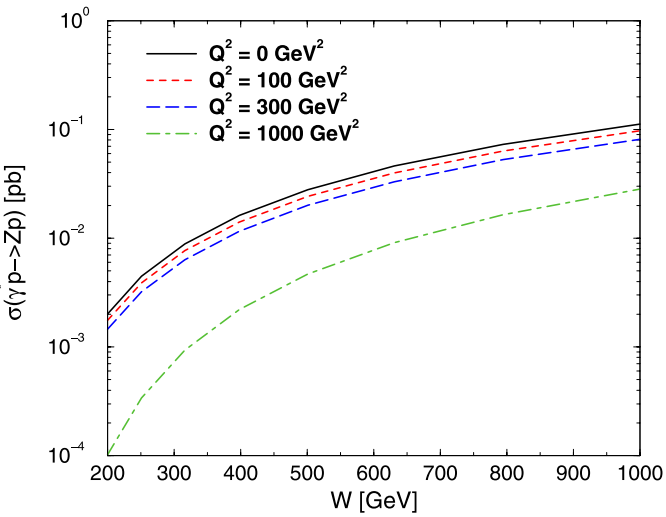

Fig. 1. The total cross section (integrated over $|t| \leq 1$) for diffractive Z^0 production in DIS as a function of energy for several photon virtualities (see text)

large mass of the Z^0, which determines the hard scale in combination with Q^2. It is only for very large Q^2 that the latter scale determines the behavior of the cross section. In order to account for the correct behavior near the Z^0 threshold production region, we have multiplied the total cross section by a factor $(1-\bar{x})^5$, where $\bar{x} = (M_{Z^0} + m_p)^2/W^2$. Notice that the photoproduction cross section for $W \gg M_{Z^0}$ can be parameterized as $\sigma_{\rm tot}(\gamma p \to Z^0 p) \approx 2 \times 10^{-4}\,{\rm fb}\,({\rm W/GeV})^{1.9}$. We emphasize that the magnitude of this cross section implies that the study of the Z^0 production is a hard task in the next generation of ep colliders. Let us now discuss the uncertainties in the present approach. As we have considered a generalization of the color dipole formalism for the scattering process, the main uncertainties come from the considered phenomenological (saturation) model parameters (λ, σ_0, γ_s), which we have taken from fits to ep HERA data. These parameters are well determined from collider data and differ by a few percents in comparison of recent implementations of the dipole cross section; see (6). The dipole picture is particularly suitable for a qualitative analysis as the physical interpretation is clear in this representation. For instance, taking (3) and the explicit expression for the overlap of wave functions, we see that the main contribution of the dipole transverse size comes from the interval $0 \leq r \leq 2/M_Z$. This fact simplifies the integration on longitudinal momentum z and the process is dominated by the so called symmetric dipole configurations. If the characteristic size of the $q\bar{q}$ pair is much smaller than the mean distance between partons, $R_0(x) = 1/Q_{\rm sat}$, then the forward scattering amplitude reads

$$\mathcal{A}^{\gamma^* h \to Z^0 h} = \int_0^\infty {\rm d}^2\mathbf{r} \int_0^1 {\rm d}z (\Psi^*_{Z^0}\Psi_{\gamma^*}) \mathcal{A}_{q\bar{q}}(x, r, \Delta = 0) \propto \int_0^{\frac{4}{M_Z^2}} {\rm d}\mathbf{r}^2 \frac{N(x,\mathbf{r}^2)}{\mathbf{r}^2} \approx \int_0^{\frac{4}{M_Z^2}} \frac{{\rm d}\mathbf{r}^2}{\mathbf{r}^2} \left(\frac{r^2 Q_{\rm sat}^2}{4}\right)^{\gamma_{\rm eff}}, \quad (7)$$

where $\gamma_{\rm eff} = \gamma_s + \frac{1}{\kappa\lambda Y} \ln \frac{2}{r Q_{\rm sat}}$. The solution for the integral above is given by

$$\mathcal{A}^{\gamma h \to Z^0 h}(x, \Delta = 0) \propto \sqrt{2\kappa\lambda Y} \left(\frac{1}{x}\right)^{\frac{\gamma_s^2 \kappa\lambda}{2}} [1 + {\rm erf}(\eta)], \quad (8)$$

with $\eta = \sqrt{1/2\kappa\lambda Y}[\ln(Q_{\rm sat}^2/M_Z^2) - \gamma_s]$. Therefore, the effective energy power for the amplitude is given by $\lambda_{\rm eff} = \gamma_s^2 \kappa\lambda/2$. Using the parameters in the model in [26] one has $\lambda_{\rm eff} \simeq 0.5$, which is consistent with the value obtained in our full numerical calculation.

Finally, we discuss the case of the photonuclear reaction $\gamma A \to Z^0 A$. A simple assumption would be to use the forward scattering amplitude scaling with the number of nucleons, A, due to no absorption occurring for dipoles with a very small transverse size. For this purpose we will rely on the geometric scaling property of the saturation models within the color dipole approach [23–25]. Following the procedure from [33], which successfully describes small-x data for ep and eA scattering, we replace $R_p \to R_A$ and $Q^2_{{\rm sat},p} \to (AR_p^2/R_A^2)^\epsilon Q^2_{{\rm sat},p}$ in (5). Basically, the saturation scale in the nucleus grows with the quotient of the transverse parton densities to the power ϵ, where $\epsilon = 1.27$ as determined by the fit to the lepton–nucleus data [33]. As an example, we get for $W \gg M_Z$ the coherent Z production cross sections $\sigma_{\rm tot}(\gamma{\rm Pb} \to Z^0{\rm Pb}) \approx 1\,{\rm fb}\,(W/{\rm GeV})^{1.8}$ and $\sigma_{\rm tot}(\gamma{\rm Ca} \to Z^0{\rm Ca}) \approx 7 \times 10^{-2}\,{\rm fb}\,(W/{\rm GeV})^{1.9}$, respectively. For the nuclear dependence, due to the geometric scaling property it can be shown that $\sigma(\gamma A \to Z^0 A) \propto [\pi R_A^2 Q^2_{{\rm sat},A}]^2/B \approx A^{\frac{2}{3}(1+\epsilon)} W^{4\lambda}$, where $B \propto R_A^2$ is the t-slope for the nuclear scattering. This is consistent with no absorption, as referred before. In what follows we will use the calculation presented above to compute diffractive Z^0 photoproduction in pp and AA collisions. In these reactions, the rapidity distribution for Z production is directly related to the cross section discussed here.

3 Photoproduction of Z^0 in coherent collisions

Let us consider the hadron–hadron interaction at large impact parameter ($b > R_{h_1} + R_{h_2}$) and at ultra-relativistic energies. In this regime we expect the electromagnetic interaction to be dominant. In heavy ion colliders, the heavy nuclei give rise to strong electromagnetic fields due to the coherent action of all protons in the nucleus, which can interact with each other. In a similar way, it also occurs when considering ultra-relativistic protons in $pp(\bar{p})$ colliders [6, 7]. The cross section for the diffractive Z^0 photoproduction in a coherent hadron–hadron collision is given in (1). For related works in coherent interactions, see [34–39]. Considering the requirement that photoproduction is not accompanied by a hadronic interaction (ultraperipheral collision) an analytic approximation for the equivalent photon flux of a nuclei can be calculated, which is given by [6, 7]

$$\frac{{\rm d}N_\gamma(\omega)}{{\rm d}\omega} = \frac{2Z^2\alpha_{\rm em}}{\pi\omega}\left[\bar{\eta}K_0(\bar{\eta})K_1(\bar{\eta}) + \frac{\bar{\eta}^2}{2}\mathcal{U}(\bar{\eta})\right], \quad (9)$$

where ω is the photon energy, $\gamma_{\rm L}$ is the Lorentz boost of a single beam and $\eta = \omega b/\gamma_{\rm L}$; $K_0(\eta)$ and $K_1(\eta)$ are the modified Bessel functions. Moreover, $\bar{\eta} = 2\omega R_A/\gamma_{\rm L}$ and $\mathcal{U}(\bar{\eta}) = K_1^2(\bar{\eta}) - K_0^2(\bar{\eta})$. Equation (9) will be used in our calculations of Z production in AA collisions. On the other hand, for proton–proton interactions, we assume that the photon spectrum is given by [40]. The coherence condition limits the photon virtuality to very low values, which implies that for most purposes, they can be considered as real. Moreover, if we consider pp/PbPb collisions at LHC, the Lorentz factor is $\gamma_{\rm L} = 7455/2930$, giving the maximum c.m.s. γN energy $W_{\gamma p} \approx 8390/950\,{\rm GeV}$. Finally, since photon emission is coherent over the entire nucleus and the photon is colorless we expect the events to be characterized by two rapidity gaps. Therefore, we see that, distinctly from central collisions, in ultraperipheral collisions the diffractive Z^0 production should occur in a clean environment in which the hadronic background is reduced.

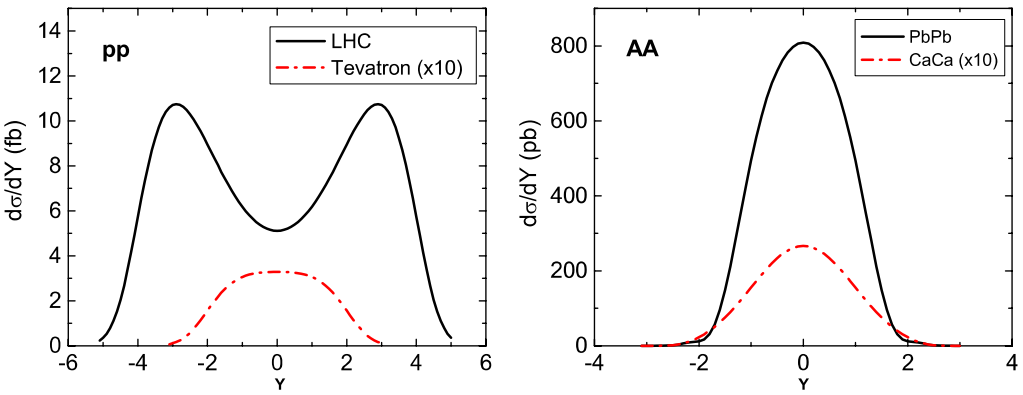

Fig. 2. The rapidity distribution for diffractive Z^0 photoproduction in pp and AA collisions (see text)

Let us calculate the rapidity distribution and total cross sections for Z^0 boson production in coherent hadron–hadron collisions, given by

$$\frac{\mathrm{d}\sigma\left[h_1+h_2\to h_1\otimes Z^0\otimes h_2\right]}{\mathrm{d}Y}=\omega\frac{\mathrm{d}N_\gamma(\omega)}{\mathrm{d}\omega}\sigma_{\gamma h\to Z^0 h}(\omega)\,, \tag{10}$$

where $Y\propto\ln(2\omega/m_{Z^0})$ and $\otimes$ represents the presence of a rapidity gap. Consequently, given the photon flux, the rapidity distribution is thus a direct measure of the photoproduction cross section for a given energy. In Fig. 2 we present respectively our predictions for Z^0 production in coherent pp (left panel) and AA (right panel) collisions. For the pp case, energies of Tevatron and LHC are considered. For AA collisions, we consider only the LHC energy and compute the cross section for light (Ca) and heavy (Pb) nuclei. We summarize the integrated cross sections in Table 1 for the LHC case, considering integration over the whole rapidity and the conservative range $|y|\leq 1$. For completeness, we quote the results for the $p\bar{p}$ Tevatron energy: for the total rapidity one has 1.3 fb, and 0.7 fb for a rapidity with $|y|\leq 1$. Assuming $\mathcal{L}=2\times10^5\,\mathrm{mb}^{-1}\,\mathrm{s}^{-1}$ at Tevatron, it implies that the corresponding events rates/s is $2.6\times10^{-7}\,\mathrm{s}^{-1}$. These results indicate that the experimental analysis of this process could be feasible only at the LHC for the pp mode. However, a more detailed discussion of the identification of the outgoing Z^0 and its main backgrounds is necessary. One sees that the main Z^0 decay mode is the hadronic one, but it is expected to be difficult to identify, due to the background from photoproduction of dijets. The magnitude of the cross section of this process in coherent interactions still is an open question, as well as its transverse momentum distribution. It needs to be studied before one can assess the observability of hadronic Z^0 decays. In other words, a comparison between the characteristics of the two final states deserves more detailed studies, which we postpone to a future publication. Consequently, in principle, the experimental search of the Z^0 would have to rely on the clean leptonic Z^0 decay modes ($Z^0\to l^+l^-$). It implies the suppression of the rate by a factor 0.7 (6.7% for the leptonic branching ratio, i.e. $Z\to e^+e^-,\mu^+\mu^-$), which reduces in approximately one order of magnitude the values presented in the Table 1. This gives ≈ 500 events/year in pp at the LHC after including branching. Consequently, if we only consider the leptonic decays of the Z^0, the separation of this process in coherent pp interactions is almost impossible. Finally, the scenario for the AA mode is pessimistic, giving very small event rates. This case also presents the additional disadvantage of having a smaller running time than the pp case, which diminishes the event rates per year. As a final comment on the order of magnitude for weak boson production we call attention for the exclusive $W^\pm$ photoproduction. It is by a factor 3 larger than Z^0 and the final state is quite interesting. Namely, now we have the main decay $W\to l\nu$, with the signal given by a single lepton and missing p_{T} (neutrino). In addition, a neutron is detected in the hadron vertex.

Table 1. The integrated cross section (event rates/s) for diffractive Z^0 photoproduction in pp/CaCa/PbPb collisions at LHC energies

h_1h_2	Total	$\lvert y\rvert<1$
PbPb ($\mathcal{L}=0.42\,\mathrm{mb}^{-1}\,\mathrm{s}^{-1}$)	1.8 nb ($0.8\times10^{-6}\,\mathrm{s}^{-1}$)	1.5 nb
CaCa ($\mathcal{L}=43\,\mathrm{mb}^{-1}\,\mathrm{s}^{-1}$)	63 pb ($2.7\times10^{-6}\,\mathrm{s}^{-1}$)	48 pb
pp ($\mathcal{L}=10^7\,\mathrm{mb}^{-1}\,\mathrm{s}^{-1}$)	69 fb ($6.8\times10^{-4}\,\mathrm{s}^{-1}$)	12 fb

Let us now discuss some of the main backgrounds. The Z^0 bosons can also be produced in inclusive hadron–hadron interactions. In comparison with inclusive Z^0 production, which is characterized by the process $h_1+h_2\to Z^0+X$, one has a photoproduction cross section smaller by approximately three orders of magnitudes for proton–proton collisions. For nuclear collisions, this factor is smaller due to hte presence of shadowing corrections (see e.g. [41]). Although the photoproduction cross section would be a small factor of the hadronic cross section, the separation of this channel is feasible if we impose the presence of two rapidity gaps in the final state. This should eliminate almost all of the hadroproduction events, while retaining most of the photoproduction interactions. However, two rapidity gaps in the final state can also be generated in hadron–hadron interactions via WW fusion, but in this case they are accompanied by two forward jets, which can be used to discriminate between the two processes. Moreover, the processes mediated by a photon implies a distinct transverse momentum distribution, which can

be used to separate the diffractive photoproduction [6, 7]. Another background process is the production of electron–positron pairs. Due to their small mass, they are produced copiously, predominantly at low invariant mass and energies and in the forward and backward direction [42]. In contrast, in leptonic Z^0 decays, the pair has an invariant mass equal to Z^0 mass and hence there are very large individual transverse momenta.

4 Summary

The study of the Z^0 production and related physics has contributed significantly for the understanding of the standard model as well as for the search of new physics. At LHC energies it should be produced copiously in pp and AA collisions. However, due to the overwhelming background of QCD multi-jet production, it is almost impossible to study the physics of hadronic Z^0 decays in central collisions. In this letter we propose to study diffractive Z^0 photoproduction in coherent hadron–hadron interactions, which is characterized by a clean environment in which the Z^0 boson produced is separated of the outgoing hadrons by rapidity gaps. This process could be tested using the forward proton detectors proposed for the CMS and ATLAS experiments at LHC. We have generalized the description of the DVCS process for Z^0 production and estimated the total cross section for the exclusive process $\gamma^* h \to Z^0 h$ ($h = p, A$) for different energies, photon virtualities and atomic numbers. Finally, we have calculated the $hh \to hZ^0h$ process and obtained the result that the experimental analyses of this process using the leptonic Z^0 decay mode is a hard task in coherent hadron–hadron collisions at LHC. The feasibility seems to be worst in ultraperipheral heavy ion collisions. However, if it were possible to separate the hadronic Z^0 decay from the background of dijet photoproduction, the analyses of exclusive Z^0 production could be feasible in pp collisions at the LHC.

Acknowledgements. The authors are grateful to Mike Albrow for calling attention to an inconsistency in the overall normalization of elementary cross sections in the previous calculation, and David dÉnterria for useful comments. This work was financed by the Brazilian funding agencies CNPq and FAPERGS.

References

1. J. Ellis, Acta Phys. Pol. B **38**, 1071 (2007)
2. J. Ellis, Nature **448**, 297 (2007)
3. J.R. Forshaw, PoS **DIFF2006**, 055 (2006) [arXiv:hep-ph/0611274]
4. M.W. Grunewald, arXiv:0710.2838 [hep-ex]
5. A.D. Martin, R.G. Roberts, W.J. Stirling, R.S. Thorne, Eur. Phys. J. C **14**, 133 (2000)
6. G. Baur, K. Hencken, D. Trautmann, S. Sadovsky, Y. Kharlov, Phys. Rep. **364**, 359 (2002)
7. C.A. Bertulani, S.R. Klein, J. Nystrand, Ann. Rev. Nucl. Part. Sci. **55**, 271 (2005)
8. A. De Roeck, in: J. Bartels et al., arXiv:0712.3633 [hep-ph], p. 181
9. M. Tasevsky, in: J. Bartels et al., arXiv:0712.3633 [hep-ph], p. 145
10. A. Hamilton, in: J. Bartels et al., arXiv:0712.3633 [hep-ph], p. 160
11. N.N. Nikolaev, B.G. Zakharov, Z. Phys. C **49**, 607 (1991)
12. N.N. Nikolaev, B.G. Zakharov, Z. Phys. C **53**, 331 (1992)
13. A.H. Mueller, Nucl. Phys. B **415**, 373 (1994)
14. M. McDermott, R. Sandapen, G. Shaw, Eur. Phys. J. C **22**, 655 (2002)
15. L. Favart, M.V.T. Machado, Eur. Phys. J. C **29**, 365 (2003)
16. L. Favart, M.V.T. Machado, Eur. Phys. J. C **34**, 429 (2004)
17. J.R. Forshaw, R. Sandapen, G. Shaw, JHEP **0611**, 025 (2006)
18. L. Favart, M.V.T. Machado, Eur. Phys. J. C **29**, 365 (2003)
19. L. Favart, M.V.T. Machado, Eur. Phys. J. C **34**, 429 (2004)
20. C. Marquet, R. Peschanski, G. Soyez, Phys. Rev. D **76**, 034011 (2007)
21. H. Kowalski, D. Teaney, Phys. Rev. D **68**, 114005 (2003)
22. J. Bartels, K.J. Golec-Biernat, K. Peters, Acta Phys. Pol. B **34**, 3051 (2003)
23. E. Iancu, R. Venugopalan, arXiv:hep-ph/0303204
24. H. Weigert, Prog. Part. Nucl. Phys. **55**, 461 (2005)
25. J. Jalilian-Marian, Y.V. Kovchegov, Prog. Part. Nucl. Phys. **56**, 104 (2006)
26. E. Iancu, K. Itakura, S. Munier, Phys. Lett. B **590**, 199 (2004)
27. K. Peters, G.P. Vacca, Eur. Phys. J. C **30**, 345 (2003)
28. R. Fiore, V.R. Zoller, JETP Lett. **82**, 385 (2005)
29. R. Fiore, Phys. Lett. B **632**, 87 (2006)
30. J. Bartels, M. Loewe, Z. Phys. **C12**, 263 (1982)
31. J. Pumplin, arXiv:9612356 [hep-ph]
32. E.R. Berger, M. Diehl, B. Pire, Eur. Phys. J. C **23**, 675 (2002)
33. N. Armesto, C.A. Salgado, U.A. Wiedemann, Phys. Rev. Lett. **94**, 022002 (2005)
34. V.P. Goncalves, M.V.T. Machado, Phys. Rev. D **77**, 014037 (2008)
35. V.P. Goncalves, M.V.T. Machado, Phys. Rev. D **75**, 031502 (2007)
36. V.P. Goncalves, M.V.T. Machado, Phys. Rev. C **73**, 044902 (2006)
37. V.P. Goncalves, M.V.T. Machado, Eur. Phys. J. C **40**, 519 (2005)
38. V.P. Goncalves, M.V.T. Machado, Phys. Rev. D **71**, 014025 (2005)
39. V.P. Goncalves, M.V.T. Machado, Eur. Phys. J. C **31**, 371 (2003)
40. M. Drees, D. Zeppenfeld, Phys. Rev. D **39**, 2536 (1989)
41. R. Vogt, Phys. Rev. C **64**, 044901 (2001)
42. G. Baur, K. Hencken, D. Trautmann, Phys. Rep. **453**, 1 (2007)